Published in final edited form as:
Bioconjug Chem. 2007 ; 18(3): 929–936.

Impact of Bidentate Chelators on Lipophilicity, Stability and Biodistribution Characteristics of Cationic ^{99m}Tc-Nitrido Complexes

Shuang Liu[*], **Zhengjie He**, **Wen-Yuan Hsieh**, and **Yong-Seung Kim**

Abstract

This report describes synthesis and evaluation of novel cationic ^{99m}Tc-nitrido complexes, [^{99m}TcN(L)(PNP)]$^+$ (L = ma, ema, tma, etma and mpo; PNP = PNP5, PNP6 and L6), as potential radiotracers for heart imaging. Cationic complexes [^{99m}TcN(L)(PNP)]$^+$ were prepared in two steps. For example, reaction of succinic dihydrazide with $^{99m}TcO_4^-$ in the presence of excess stannous chloride and PDTA resulted in the [^{99m}TcN(PDTA)$_n$] intermediate, which then reacted Hmpo and PNP6 at 100 °C for 10 – 15 min to give [^{99m}TcN(mpo)(PNP6)]$^+$ in >90% yield. It was found that bidentate chelators have a significant impact on lipophilicity, solution stability, biodistribution and metabolic stability of cationic ^{99m}Tc-nitrido complexes. The fact that [^{99m}TcN(ema)(PNP6)]$^+$ decomposes rapidly in presence of cysteine (1 mg/mL) while [^{99m}TcN(etma)(PNP6)]$^+$ and [^{99m}TcN(mpo)(PNP6)]$^+$ remain stable for >6 h under the same conditions strongly suggests that thione-S donors in bidentate chelators increase the solution stability of their cationic ^{99m}Tc-nitrido complexes. Biodistribution studies were performed on four cationic ^{99m}Tc-nitrido complexes in Sprague-Dawley rats. [^{99m}TcN(etma)(PNP5)]$^+$ is of particular interest due to its high initial heart uptake (1.81±0.35 %ID/g at 5 min postinjection), and long myocardial retention (1.99±0.47 %ID/g at 120 min postinjection). The heart/liver ratio of [^{99m}TcN(etma)(PNP5)]$^+$ (6.06±1.48) at 30 min postinjection is almost identical that of ^{99m}TcN-DBODC5 (6.01±1.45), and is >2 times better than that of ^{99m}Tc-sestamibi (2.90±0.22). Results from metabolism studies show that [^{99m}TcN(etma)(PNP5)]$^+$ has no significant metabolism in the urine; but it does show significant metabolism in feces samples at 120 min postinjection. Planar imaging studies suggest that [^{99m}TcN(etma)(PNP5)]$^+$ might be able to give clinically useful images of the heart as early as 30 min postinjection. [^{99m}TcN(etma)(PNP5)]$^+$ is a very promising candidate for more pre-clinical evaluations in various animal models.

INTRODUCTION

Recently, we reported a series of crown ether-containing cationic complexes [^{99m}TcN(DTC)(PNP)]$^+$ (Figure 1: DTC = L1 – L5; PNP = PNP5 and L6) as potential radiotracers for heart imaging (1). Results from biodistribution studies have clearly demonstrated that crown ether groups are very useful for improvement of the liver clearance of cationic ^{99m}Tc-nitrido complexes, some of which have the heart uptake comparable to that of ^{99m}Tc-sestamibi, the most successful radiotracer for myocardial perfusion imaging, with the heart/liver ratios being 4 – 5 time better than that of ^{99m}Tc-sestamibi at 120 min postinjection (p.i.). Results from imaging studies suggested that they might be able to give clinically useful images of heart as early as 30 min p.i. These promising results led us to explore other bidentate chelators for preparation of cationic ^{99m}Tc-nitrido complexes that have the heart/liver ratio substantially better than that of ^{99m}Tc-sestamibi while maintaining their high heart uptake.

*To whom correspondence should be addressed. Room 1275, Civil Engineering Building, School of Health Sciences, Purdue University, 550 Stadium Mall Drive, West Lafayette, IN 47907. Phone: 765-494-0236; Fax 765-496-1377; Email: lius@pharmacy.purdue.edu.

As an extension of our previous studies, we now report the use of maltol (Hma), thiomaltol (Htma), ethylmaltol (Hema), ethylthiomaltol (Hetma), and 2-mercaptopyridine oxide (Hmpo) as the bidentate chelators for preparation of cationic complexes $[^{99m}TcN(L)(PNP)]^+$ (Figure 1: L = ma, ema, tma, etma, and mpo; PNP = PNP5, PNP6 and L6). These cationic ^{99m}Tc-nitrido complexes are designed in such a way that the lipophilicity and biodistribution characteristics can be modified by the choice of bidentate chelators and bisphosphines. Compared to the crown ether-containing DTCs (Figure 1: L1 – L5), these bidentate chelators offer a greater structural diversity, which is very important for modification of biodistribution properties of cationic ^{99m}Tc radiotracers. To demonstrate their potential as radiotracers for heart imaging, we carried out biodistribution studies on four cationic ^{99m}Tc-nitrido complexes in Sprague-Dawley rats. Results from these studies will be compared to those of ^{99m}Tc-sestamibi and ^{99m}TcN-DBODC5 (DBODC = N,N-bis(ethyoxythyl)dithiocarbamate) reportedly having the best heart/liver ratio among the known cationic ^{99m}Tc radiotracers (2–4).

It is well-documented that maltol and ethylmaltol form neutral complexes with many biologically important metal ions (5–10). Their vanadyl(IV) complexes have been reported to possess insulin enhancing activity (11–15). The Co(II), Cu(II) and Cr(III) complexes of maltol have also been studied for their anti-hypoglycemic activity (16). Recently, thiolmaltol and ethylthiomaltol and their N-substituted derivatives have been used for preparation of their Cu (II), Ni(II), Zn(II), V(IV), group 13 and lanthanide metal complexes (17–21). The study described herein represents the first one to use these bidentate chelators to prepared cationic complexes $[^{99m}TcN(L)(PNP)]^+$ (Figure 1: L = ma, ema, tma, etma, and mpo; PNP = PNP5, PNP6 and L6).

EXPERIMENTAL

Materials

Chemicals, such as 1,2-diaminopropane-N,N,N′,N′-tetraacetic acid (PDTA), maltol (Hma), ethylmaltol (Hema), and mercaptopyridine oxide (Hmpo), were purchased from *Sigma/Aldrich* (St. Louis), and were used as received. Thiomaltol (Htma) and ethylthiomaltol (Hetma) were prepared according to the literature methods (17–21). Synthesis of N-ethoxyethyl-N,N-bis[2-(bis(3-methoxypropyl)phosphino)ethyl]amine (PNP5), N-ethoxyethyl-N,N-bis[2-(bis(3-ethoxypropyl)phosphino)ethyl]amine (PNP6) and N-methoxyethyl-N,N-bis[2-(bis(3-ethoxypropyl)phosphino)ethyl]amine (L6) has been described in our previous report (1). ^{99m}TcN-DBODC5 was prepared according to the literature method (2–4). Cardiolite® vials were obtained as a gift from Bristol Myers Squibb Medical Imaging (North Billerica, MA), and were reconstituted according to the manufacturer's insert.

Methods

The radio-HPLC method used a LabAlliance semi-prep HPLC system with a β-Ram IN-US detector, and a Zorbax C_8 column (4.6 mm × 150 mm, 100 Å pore size). The flow rate was 1 mL/min. The mobile phase was isocratic with 30% solvent A (25 mM NH_4OAc buffer, pH = 6.8) and 70% solvent B (methanol) at 0 – 5 min, followed by a gradient from 70% solvent B at 5 min to and 90% solvent B at 15 min.

General Procedure for Preparation of Cationic ^{99m}Tc-Nitrido Complexes

The solution containing SDH and PDTA was prepared according to the procedure described in our previous communication (1). To a 5 cc vial were added 1.0 mL of the solution containing SDH (5 mg/mL) and PDTA (5 mg/mL), 1.0 mL of $^{99m}TcO_4^-$ solution (2 – 10 mCi), and 20 μL of $SnCl_2$ solution (1 mg in 1.0 N HCl). The reaction mixture was kept at room temperature for 15 – 30 min to form the ^{99m}Tc-nitrido intermediate. After adding 0.5 mL of the solution containing the bidentate chelator (5 – 10 mg/mL) and the bisphosphine (5 – 10 mg/mL), the

reaction mixture was heated at 95 °C for 10 – 15 min. After completion of radiolabeling, the vial was placed back into the lead pig, and allowed to stand at room temperature for 5 – 10 min. A sample of the resulting solution was analyzed by the radio-HPLC. The radiochemical purity (RCP) was >95% with minimal amount (<0.5%) of [^{99m}Tc]colloid formation.

Composition Studies

The mixed-ligand experiments were performed to determine the number of bidentate chelators or bisphosphines in cationic ^{99m}Tc-nitrido complexes according to the method described in our previous communication (1). The radiolabeling procedure was identical to that above except that two bidentate chelators or PNP-type bisphosphines were used as competing ligands in a the same vial. For example, a mixture of Hma (2 mg) and Hema (2 mg) was used to determine the number of bidentate chelators in cationic complexes $[^{99m}TcN(L)(PNP6)]^+$. The number of bisphosphines was determined in a similar fashion using a mixture L6 (2 mg) and PNP6 (2 mg).

Doses for Animal Studies

For biodistribution studies on $[^{99m}TcN(L)(L6)]^+$ (L = ema, tma and etma) and $[^{99m}TcN(etma)(PNP5)]^+$, the radiotracer was purified by HPLC to remove all radioimpurities. Volatiles in the mobile phase were evaporated under reduced pressure. Doses were made by dissolving the residue to ~10 μCi/mL in saline with 15% (w/w) propylene glycol. The resulting solution was filtered with a 0.20 micron filter unit to eliminate particles before being injected into animals. The injection volume was 0.1 mL for each animal in biodistribution studies. For imaging studies with $[^{99m}TcN(etma)(PNP5)]^+$ was first purified by HPLC. Volatiles in the mobile phase were completely removed under the reduced pressure. Doses were made by dissolving the residue to ~2.5 mCi/mL in saline containing ~15% (w/w) propylene glycol. The injection volume was ~0.25 mL for each animal in the imaging studies.

Determination of Log P Values

Log P values of cationic ^{99m}Tc-nitrido complexes were determined using the following procedure: the ^{99m}Tc radiotracer was prepared and purified by HPLC. The collected mobile phases were evaporated and the residue was dissolved in a mixture of equal volume (3 mL:3 mL) n-octanol and 25 mM phosphate buffer (pH = 7.4). After vortex for >20 min, the mixture was centrifuged at 8,000 rpm for 5 min. Samples (in triplets) from aqueous and n-octanol were obtained and counted separately in a gamma counter (Beckman Gama 8000). The partition coefficients were calculated using the equation: P = (activity concentration in n-octanol)/(activity concentration in aqueous layer). The log P value was measured three different times and reported as an average of three different measurements.

Solution Stability

For solution stability in kit matrix, the radiotracer was prepared and analyzed by radio-HPLC at 0, 1, 2, 3, and 6 h post-labeling. For cysteine challenging experiment, the resulting reaction solution was mixed with an equal volume of a cysteine (1 mg/mL) solution. Samples of the mixture were analyzed by radio-HPLC at 0, 1, 2, 3, and 6 h.

Biodistribution Studies

Biodistribution studies were performed using Sprague-Dawley rats in compliance with NIH animal experiment guidelines (*Principles of Laboratory Animal Care*, NIH Publication No. 86-23, revised 1985). This animal model has been used as the screening tool for cationic ^{99m}Tc radiotracers (*51–56*). The protocols for these studies have been approved by the Purdue University Animal Care and Use Committee (PACUC). In short, sixteen Sprague-Dawley rats (200 – 250 g) were anesthetized with intramuscular injection of a mixture of

ketamine (80 mg/kg) and xylazine (19 mg/kg). A jugular vein was surgically exposed, and each animal was administered with 1 – 3 μCi of the purified radiotracer in 100 μL of 10 – 20% propylene glycol. Four animals were sacrificed by sodium pentobarbital overdose at each time point (5, 30, 60 and 120 min p.i.). Blood was withdrawn from the heart through a syringe. Organs of interest (heart, brain, lung, liver, spleen, kidneys, muscle and intestine) were excised, rinsed with saline, dried with tissues, weighed, and counted on a gamma counter (Beckman RD8000). Four extra doses were also weighed and counted before and after tissue samples. The organ uptake was calculated as a percentage of the injected dose per gram of wet tissue mass (%ID/g) and a percentage of the injected dose per wet organ (%ID/organ). The biodistribution data and T/B ratios are reported as an average plus the standard variation.

Imaging Studies

Two Sprague-Dawley rats (200 – 250 g) were anesthetized with intramuscular injection of a mixture of ketamine (80 mg/kg) and xylazine (19 mg/kg). The radiotracer (300 – 500 μCi) was administered via surgically exposed jugular vein. Animals will be monitored on the gamma camera (PhoGama large field-of-view Anger camera and NucLearMac computer system). Sequential anterior images were collected for 5 min at the specified time (5, 15, 30, 60 min and 120 min) using 256 × 256 image matrix while animal are still under anesthesia. Images of rats administered with ^{99m}Tc-sestamibi and ^{99m}TcN-DBODC5 were obtained using the same protocol. After imaging, the animals were sacrificed by sodium pentobarbital overdose. The urine and feces samples were collected for metabolism studies.

Metabolism

The urine samples were collected from the rats at 30 and 120 min p.i. by manual void, and were mixed with equal volume of acetonitrile. The mixture was centrifuged at a speed of 8,000 rpm. The supernatant was collected and filtered through a 0.20 micron Millex-LG syringe driven filter unit. The filtrate was analyzed by radio-HPLC. The feces samples were collected once they were sacrificed after the imaging study (at ~120 min p.i.). The sample was suspended in a mixture of 50% acetonitrile aqueous solution, and the resulting mixture was vortexed for 5 – 10 min. After centrifuging, the supernatant was collected and passed through a 0.20 μfilter. The filtrate was analyzed by radio-HPLC.

Data and Statistical Analysis

The biodistribution data and T/B ratios are reported as an average plus the standard variation based on the results from four animals for each time point. Comparison between two different radiotracers was made using the one-way ANOVA test. The level of significance was set at $p = 0.05$.

RESULTS

Radiochemistry

Cationic complexes $[^{99m}TcN(L)(PNP)]^+$ (L = ma, ema, tma, etma and mpo; PNP = PNP5, PNP6 and L6) were prepared according to Scheme I. First, $^{99m}TcO_4^-$ was allowed to react with SDH in the presence of excess PDTA and stannous chloride. The reaction mixture was allowed to stand at room temperature for 15 – 30 min to form the $[^{99m}TcN(PDTA)_n]$ intermediate, which was then reacted with the bidentate chelator and bisphosphine at 100 °C for 10 – 15 min to give the cationic complex $[^{99m}TcN(L)(PNP)]^+$ (L = ma, ema, tma, etma and mpo; PNP = PNP5, PNP6 and L6). Using this procedure, all new radiotracers had >85% RCP with minimal amount (<0.5%) of [^{99m}Tc]colloid formation.

A reversed phase radio-HPLC method was used to analyze cationic complexes $[^{99m}TcN(L)(PNP)]^+$ (L = ma, ema, tma, etma, and mpo; PNP = PNP5, PNP6 and L6). Their HPLC retention times are listed in Table 1. Figure 2 illustrates representitive radio-HPLC chromatograms of $[^{99m}TcN(ma)(PNP6)]^+$ and $[^{99m}TcN(ema)(PNP6)]^+$. There is always an impurity peak (5 – 10%) in their radio-HPLC chromatograms. These radioimpurities are most likely due to partial oxidation of the bisphosphine ligand during preparation or radiolabeling. This explanation is supported by the fact that the radioimpurities could be totally eliminated when the extra pure bisphosphine was used for the radiolabeling.

The mixed-ligand experiment was performed to determine the composition (the number of bidentate chelators and bisphosphine ligands) of cationic ^{99m}Tc-nitrido complexes. In the first experiment, we used PNP6 as the bisphosphine ligand, Hma and Hema as the competing chelators. After radiolabeling, the reaction mixture was analyzed by radio-HPLC. Figure 3 shows the typical radio-HPLC chromatogram of the reaction mixture containing $[^{99m}TcN(ma)(PNP6)]^+$ and $[^{99m}TcN(ema)(PNP6)]^+$. If only one bidentate chelator is bonded to the Tc, the HPLC chromatogram should show two peaks: one from $[^{99m}TcN(ma)(PNP6)]^+$ and the other from $[^{99m}TcN(ema)(PNP6)]^+$. If two bidentate chelators were bonded to the Tc, there would have been a third peak from the mixed-ligand complex, $[^{99m}TcN(ma)(ema)(PNP6)]$. The presence of two distinctive peaks at ~14.5 min and ~16.5 min for $[^{99m}TcN(ma)(PNP6)]^+$ and $[^{99m}TcN(ema)(PNP6)]^+$, respectively, clearly demonstrates that there is only one bidentate chelator in cationic complex $[^{99m}TcN(L)(PNP)]^+$. The number of bisphosphines in cationic complex $[^{99m}TcN(L)(PNP)]^+$ was determined in a similar fashion using Hema as the bidentate chelator, L6 and PNP6 as the competing ligands. Figure 4 shows the radio-HPLC chromatogram of the resulting reaction mixture containing $[^{99m}TcN(ema)(L6)]^+$ and $[^{99m}TcN(ema)(PNP6)]^+$. The peaks at 14.0 min is due to $[^{99m}TcN(ema)(L6)]^+$ and the peak at 15.5 min is from $[^{99m}TcN(ema)(PNP6)]^+$. This clearly demonstrates that there is only one bisphosphine in $[^{99m}TcN(L)(PNP)]^+$. Once again, the radioimpurities (~20%) at 10 – 12 min are caused by the partial oxidation of PNP6 during preparation.

We studied the solution stability of $[^{99m}TcN(L)(PNP)]^+$ (L = ma, ema, tma, etma and mpo; PNP = PNP5, PNP6 and L6) in the kit matrix and after purification. It was found that they all remain stable for more than 6 h. The cysteine challenge experiment was also performed for $[^{99m}TcN(L)(PNP6)]^+$ (L = ema, etma and mpo). It was found that $[^{99m}TcN(ema)(PNP6)]^+$ decomposes rapidly in the presence of cysteine (~1.0 mg/mL). The RCP was >90% in the kit matrix and decreased to 61.6% at 2 h and 30.1% at 6 h (Figure 5). In contrast, $[^{99m}TcN(etma)(PNP6)]^+$ and $[^{99m}TcN(mpo)(PNP6)]^+$ remain stable (>6 h) in presence of excess cysteine (1.0 mg/mL) at ambient temperature (Figure 5). The use of thione-S donors in bidentate chelators increases solution stability of their cationic ^{99m}Tc-nitrido complexes.

Lipophilicity plays a significant role in the heart uptake and excretion kinetics of cationic ^{99m}Tc radiotracers (1,22–25). Thus, it is important to explore the impact of bidentate chelators and bisphosphines on lipophilicity of their cationic ^{99m}Tc-nitrido complexes. Partition coefficient constants of $[^{99m}TcN(L)(PNP)]^+$ (L = ma, ema, tma, etma and mpo; PNP = PNP5, PNP6 and L6) were determined by measuring their distribution in a mixture of equal volume n-octanol and 25 mM phosphate buffer (pH = 7.4). HPLC purification was needed to minimize the interference from other radioimpurities. The log P values are summarized in Table 1. In general, cationic complexes $[^{99m}TcN(L)(PNP)]^+$ (L = ma and tma) have lower lipophilicity than $[^{99m}TcN(L)(PNP)]^+$ (L = ema and etma) due to the extra methylene group. $[^{99m}TcN(L)(PNP)]^+$ (L = tma and etma) are more lipophilic than $[^{99m}TcN(L)(PNP)]^+$ (L = ma and ema) due to the presence of thione-S donor. $[^{99m}TcN(L)(PNP6)]^+$ is more lipophilic than $[^{99m}TcN(L)(PNP5)]^+$ due to the presence of four ethoxypropyl groups in PNP6 instead of four methoxypropyl groups in PNP5. The lipophilicity of $[^{99m}TcN(mpo)(PNP)]^+$ is between that of $[^{99m}TcN(tma)(PNP)]^+$ and $[^{99m}TcN(etma)(PNP)]^+$.

Biodistribution Characteristics

Biodistribution studies in rats were performed on [^{99m}TcN(etma)(PNP5)]$^+$, [^{99m}TcN(ema)(L6)]$^+$, [^{99m}TcN(tma)(L6)]$^+$, and [^{99m}TcN(etma)(L6)]$^+$. We choose these four radiotracers to demonstrate the impact of the solution stability and lipophilicity on their biodistribution characteristics. The biodistribution data and T/B ratios are listed in Tables SI – SIV. Figure 7 shows the direct comparison of heart uptake and heart/liver ratios with ^{99m}Tc-Sestamibi and ^{99m}TcN-DBODC5. Biodistribution data for ^{99m}Tc-Sestamibi and ^{99m}TcN-DBODC5 in the same animal model were obtained from our previous report (1).

[^{99m}TcN(ema)(L6)]$^+$ has a lop P value of 1.22±0.13, which is almost identical to that of ^{99m}Tc-Sestamibi (1.29±0.13). It had a moderate heart uptake (1.58±0.41 %ID/g at 5 min p.i. and 1.60±0.48 %ID/g at 120 min p.i.) with the heart/liver ratios being 0.35±0.04, 1.06±0.34, 2.56±0.23, and 5.43±1.37 at 5, 30, 60 and 120 min p.i., respectively. [^{99m}TcN(etma)(L6)]$^+$ has the log P of 1.43±0.05. It has a low heart uptake (1.10±0.10 %ID/g at 5 min p.i. and 1.27±0.51 %ID/g at 120 min p.i.) and poor heart/liver ratios (0.37±0.01, 1.21±0.16, 1.17±0.19, and 1.91 ±0.31 at 5, 30, 60 and 120 min p.i., respectively). [^{99m}TcN(tma)(L6)]$^+$ has the log P value (1.09 ±0.17) that is almost identical to that of ^{99m}TcN-DBODC5 (1.10±0.07). It shows a high initial heart uptake (2.03±0.75 %ID/g at 5 min p.i.) with a long myocardial retention (2.01±0.40 % ID/g at 120 min p.i.). Its heart/liver ratios are 1.10±0.09, 2.01±0.41, 3.55±0.34, and 6.25±0.68 at 5, 30, 60 and 120 min p.i., respectively. The log P value of [^{99m}TcN(etma)(PNP5)]$^+$ is 0.67 ±0.15. It has a relatively high heart uptake (1.81±0.35 %ID/g at 5 min p.i.), a long myocardial retention (1.99±0.47 %ID/g at 120 min p.i.), and high heart/liver ratios (6.06±0.90, 10.36±2.25, and 16.46±4.24 at 30, 60 and 120 min p.i., respectively).

Imaging Studies

[^{99m}TcN(etma)(PNP5)]$^+$ was chosen for the imaging study in rats due to its much better heart/liver ratios than those of ^{99m}Tc-Sestamibi. For comparison purpose, we also obtained images of rats administered with ^{99m}Tc-sestamibi and ^{99m}TcN-DBODC5. Figure 7 illustrates planar images of rats administered with [^{99m}TcN(etma)(PNP5)]$^+$, ^{99m}Tc-Sestamibi and ^{99m}TcN-DBODC5. In general, all the images acquired at 5 min p.i. show a very high liver uptake adjacent to the heart; but the lung activity was low for all three radiotracers. At 30 min p.i., the liver activity for [^{99m}TcN(etma)(PNP5)]$^+$ and ^{99m}TcN-DBODC5 is reduced significantly. By 60 min p.i., the liver activity almost disappeared for [^{99m}TcN(etma)(PNP5)]$^+$ and ^{99m}TcN-DBODC5 while the liver activity level for ^{99m}Tc-Sestamibi remained high.

Metabolism

We examined metabolism of [^{99m}TcN(etma)(PNP5)]$^+$ by analyzing the urine and feces samples from the rats used in imaging studies. Figure 8 shows its radio-HPLC chromatograms in the kit matrix (A), in urine at 30 min p.i. (B), in urine at 120 min p.i. (C), and in feces at 120 min p.i. (D). Obviously, very small amount of metabolite was detected in the urine samples (Figure 8: B and C); but a significant metabolism was observed in feces samples of rats administered with [^{99m}TcN(etma)(PNP5)]$^+$ (Figure 8D).

DISCUSSION

Myocardial perfusion imaging with radiotracers is an integral component of the clinical evaluation of patients with known or suspected coronary artery disease (26–29). Since the early 1980s, intensive research efforts have been directed towards development of cationic ^{99m}Tc complex radiotracers for heart imaging (26,27). As a result these efforts, ^{99m}Tc-Sestamibi and ^{99m}Tc-Tetrofosmin have been approved as commercial products for myocardial perfusion imaging. Despite their widespread applications, both ^{99m}Tc-Sestamibi and ^{99m}Tc-Tetrofosmin do not meet the requirements of an ideal perfusion imaging agent, at least in part, due to their

high liver uptake (30). Therefore, it would be a great advantage to develop a new radiotracer with substantially better heart/liver ratio than that of ^{99m}Tc-Sestamibi.

The factors affecting biodistribution patterns of radiotracers include the charge, solution stability, lipophilicity, and protein-binding capability. For example, $[^{99m}TcN(ema)(L6)]^+$ and ^{99m}Tc-Sestamibi share the same cationic charge, and have very high lipophilicity (1.22 ±0.13 and 1.29±0.13, respectively). However, the heart uptake and heart/liver ratios of $[^{99m}TcN(tma)(L6)]^+$ are significantly lower ($P<0.01$) than that of ^{99m}Tc-Sestamibi at 5 – 60 min postinjection. This difference is probably related to its solution instability of $[^{99m}TcN(ema)(L6)]^+$ in the presence of cysteine (Figure 6). The solution instability of $[^{99m}TcN(ema)(L6)]^+$ may also contribute to its high protein binding as indicated by its relatively high blood activity and low heart/blood ratios (Table SIII).

Compared to $[^{99m}TcN(ema)(L6)]^+$, $[^{99m}TcN(etma)(L6)]^+$ has better solution stability due to the thione-S donor atom in etma. However, it has a low heart uptake with low heart/lung and heart/liver ratios, suggesting that it is probably too lipophilic (log P = 1.43±0.05) to achieve the high heart uptake and fast liver clearance. $[^{99m}TcN(tma)(L6)]^+$ has a high solution stability. Its log P value is almost identical to that of ^{99m}TcN-DBODC5 (Table 1). The heart uptake of $[^{99m}TcN(tma)(L6)]^+$ is comparable to that of ^{99m}TcN-DBODC5 (Figure 6); but its heart/liver and heart/liver ratios are significantly lower ($p<0.01$) than that of ^{99m}TcN-DBODC5 over the 2 h study period. In contrast, $[^{99m}TcN(etma)(PNP5)]^+$ is less lipophilic (log P = 0.67±0.15). Its heart uptake is comparable to that of ^{99m}TcN-DBODC5 within the experimental error (Figure 6). The heart/liver ratio of $[^{99m}TcM(etma)(PNP5)]^+$ is very similar to that of ^{99m}TcN-DBODC5 at 5 – 60 min p.i.

Another important factor influencing the *in vivo* biological properties of cationic ^{99m}Tc radiotracers is their metabolic properties. Cationic ^{99m}Tc radiotracers are generally excreted via hepatobiliary and renal routes. Metabolic products can be readily detected by analyzing the urine (renal excretion) and feces (hepatobiliary excretion) samples. In this study, we used a reversed phase radio-HPLC method to analyze the urine and feces samples from the rats administered with ~500 μCi of $[^{99m}TcN(etma)(PNP5)]^+$. The results indicated that $[^{99m}TcN(etma)(PNP5)]^+$ remained intact in the urine over 2 h study period (Figure 9C); but it shows a significant metabolism (>70%) in feces samples at 120 min p.i. (Figure 9D). In contrast, ^{99m}TcN-DBODC5, which shares the same PNP5 bisphosphine ligand with $[^{99m}TcN(etma)(PNP5)]^+$, has very little metabolism in both urine and feces of rats under anesthesia (1). Changing the bidentate chelator from DBODC to ethylthiomaltolate (etma) has a significant impact on metabolic fate of the cationic ^{99m}Tc-nitrido complex. The metabolic instability of $[^{99m}TcN(etma)(PNP5)]^+$ may contribute to its lower heart/liver ratio than that of ^{99m}TcN-DBODC5 at 120 min p.i. (Figure 6).

It is well-documented that cationic ^{99m}Tc radiotracers, such as ^{99m}Tc-Sestamibi and ^{99m}Tc-Tetrofosmin, are able to penetrate plasma and mitochondrial membranes and accumulated in mitochondria because of the negative mitochondrial potential (31–35). Due to their similarity in molecular charge with ^{99m}Tc-Sestamibi and ^{99m}Tc-Tetrofosmin, it is reasonable to believe that cationic ^{99m}Tc-nitrido complexes might share the same localization mechanism. The difference in the heart uptake of cationic ^{99m}Tc radiotracers is most likely caused by their lipophilicity and capability to across the plasma and mitochondrial membranes.
Cationic ^{99m}Tc radiotracers with the log P>1.5 often have a low heart uptake and a slow liver clearance while more hydrophilic cationic radiotracers with log P<0 tend to show fast washout from the myocardium (1–3,22–25). In both cases, the heart/liver ratio is low because of either high liver uptake or fast myocardial washout. While there is no clear-cut “optimal” log P values, we believe that cationic ^{99m}Tc radiotracers should have a log P value of 0.6 – 1.2 in order to achieve a high heart uptake with the fast liver clearance at the same time.

CONCLUSIONS

This report describes synthesis and evaluation of cationic complexes $[^{99m}TcN(L)(PNP)]^+$ (Figure 1: L = ma, ema, tma, etma, and mpo; PNP = PNP5, PNP6 and L6) as potential radiotracers for heart imaging. The key finding of this study is that bidentate chelators have a significant impact on lipophilicity, solution stability, biodistribution patterns, and metabolism of their cationic ^{99m}Tc-nitrido complexes. The results from solution stability studies indicate that the thione-S donors in bidentate chelators increase solution stability of cationic ^{99m}Tc-nitrido complexes. Among four radiotracers evaluated in Sprague-Dawley rats for their biodistribution characteristics, $[^{99m}TcN(etma)(PNP5)]^+$ has a high heart uptake, long myocardial retention, and fast liver clearance with the heart/liver ratio being >2 times better than that of ^{99m}Tc-sestamibi at 30 min p.i. Results from planar imaging studies are completely consistent with those from biodistribution studies. The fast liver clearance suggests that $[^{99m}TcN(etma)(PNP5)]^+$ might give clinically useful images of heart as early as 30 min p.i. $[^{99m}TcN(etma)(PNP5)]^+$ is a promising candidate for evaluation of its blood flow characteristics in larger animal models, such as dogs and pigs. It is interesting to note that the heart/liver ratio of $[^{99m}TcN(etma)(PNP5)]^+$ is not as good as that of ^{99m}TcN-DBODC5 at 120 min p.i. probably due to its metabolic instability in the hepatobiliary system. Therefore, our future research will focus more on cationic ^{99m}Tc-nitrido complexes with better metabolic stability.

Acknowledgements

Authors would like to thank Lee Ann Grote, Carol Dowell and Cheryl Anderson from the Department of Veterinary Clinical Sciences, Purdue University, for their assistance with biodistribution and imaging studies. This work is supported, in part, by Purdue University and research grants AHA0555659Z (S.L.) from the Greater Midwest Affiliate of American Heart Association, 5 R21 EB003419-02 (S.L.) from National Institute of Biomedical Imaging and Bioengineering (NIBIB), and 1 R21 HL083961-01 (S.L.) from National Heart, Lung, and Blood Institute (NHLBI).

Abbreviations

PDTA
1,2-diaminopropane-N,N,N′,N′-tetraacetic acid

Hma
maltol

Htma
thiomaltol

Hema
ethylmaltol

Hetma
ethylthiomaltol

Hmpo
and 2-mercaptopyridine oxide

PNP5
N-ethoxyethyl-N,N-bis[2-(bis(3-methoxypropyl)phosphino)ethyl]amine

PNP6
N-ethoxyethyl-N,N-bis[2-(bis(3-ethoxypropyl)phosphino)ethyl]amine

L6
N-methoxy-ethyl-N,N-bis[2-(bis(3-ethoxypropyl)phosphino)ethyl]amine

Literature Cited

1. Liu S, He ZJ, Hsieh WY. Evaluation of novel crown ether-containing cationic ^{99m}Tc-nitrido complexes as new radiopharmaceuticals for heart imaging. Nucl Med Biol 2006;33:419–432. [PubMed: 16631092]
2. Boschi A, Bolzati C, Uccelli L, Duatti A, Benini E, Refosco F, Tisato F, Piffanelli A. A class of asymmetrical nitrido ^{99m}Tc heterocomplexes as heart imaging agents with improved biological properties. Nucl Med Commun 2002;23:689–693. [PubMed: 12089492]
3. Boschi A, Uccelli L, Bolzati C, Duatti A, Sabba N, Moretti E, Di Domenico G, Zavattini G, Refosco F, Giganti M. Synthesis and biologic evaluation of monocationic asymmetrical ^{99m}Tc-nitride heterocomplexes showing high heart uptake and improved imaging properties. J Nucl Med 2003;44:806–814. [PubMed: 12732683]
4. Hatada K, Riou LM, Ruiz M, Yamamichi Y, Duatti A, Lima RL, Goode AR, Watson DD, Beller GA, Glover DK. ^{99m}Tc-N-DBODC5, a new myocardial perfusion imaging agent with rapid liver clearance: comparison with ^{99m}Tc-Sestamibi and ^{99m}Tc-Tetrofosmin in rats. J Nucl Med 2004;45:2095–2101. [PubMed: 15585487]
5. Nelson WO, Rettig SJ, Orvig C. The exoclathrate $Al(C_7H_8NO_2)_3{\cdot}12H_2O$. A facial geometry imposed by extensive hydrogen bonding with the ice I structure. J Am Chem Soc 1987;109:4121–4123.
6. Bernstein LR, Tanner T, Godfrey C, Noll B. Chemistry and pharmacokinetics of gallium maltolate, a compound with high oral gallium bioavailability. Metal Based Drugs 2000;7:33–47. [PubMed: 18475921]
7. Matsuba CA, Nelson WO, Rettig SJ, Orvig C. Neutral water-soluble indium complexes of 3-hydroxy-4-pyrones and 3-hydroxy-4-pyridinones. Inorg Chem 1988;27:3935–3939.
8. Hsieh WY, Zaleski CM, Pecoraro VL, Liu S. Mn(II) Complexes of Monoanionic Bidentate Chelators: the X-Ray Crystal Structures of $Mn(DHA)_2(CH_3OH)_2$ (DHA = Dehydroacetic Acid) and $[Mn(ema)_2(H_2O)]_2{\cdot}2H_2O$ (Hema = 2-Ethyl-3-Hydroxy-4-Pyrone. Inorg Chim Acta 2006;359:228–236.
9. 9Hsieh WY, Liu S. Synthesis, characterization and structures of Mn(III) complexes $Mn(DMHP)_3{\cdot}12H_2O$ and $Mn(DMHP)_2Cl{\cdot}0.5H_2O$ (DMHP = 1,2-dimethyl-3-hydroxy-4-pyridinone). Inorg Chem 2005;44:2031–2038. [PubMed: 15762730]
10. Hsieh WY, Liu S. Synthesis, characterization and structures of Cr(III) complexes with 3-hydroxy-4-pyrones and 1,2-dimethyl-3-hydroxy-4-pyridinone. Synthesis and Reactivity In Inorganic, Metal-Organic and Nano-Metal Compounds 2005;35:61–70.
11. McNeill JH, Yuen VG, Hoveyda HR, Orvig C. Bis(maltolato)-oxovanadium(IV) is a potent insulin mimic. J Med Chem 1992;35:1489–1491. [PubMed: 1573642]
12. Caravan P, Gelmini L, Glover N, Herring FG, Li HL, McNeill JH, Rettig SJ, Setyawati IA, Shuter E, Sun Y, Tracey AS, Yuen VG, Orvig C. Reaction chemistry of BMOV, bis(maltolato)oxovanadium (IV), a potent insulin mimetic agent. J Am Chem Soc 1995;117:12759–12770.
13. Thompson KH, Orvig C. Coordination chemistry of vanadium in metallopharmaceutical candidate compounds. Coord Chem Rev 2001;219:1033–1053.references therein
14. Thompson KH, Orvig C. Design of vanadium compounds as insulin enhancing agents. J Chem Soc, Dalton Trans 2000:2885–2892.references therein
15. Saatchi K, Thompson KH, Patrick BO, Pink M, Yuen VG, McNeill JH, Orvig C. Coordination chemistry and insulin-enhancing behavior of vanadium complexes with maltol $C_6H_6O_3$ Structural isomers. Inorg Chem 2005;44:2689–2697. [PubMed: 15819554]
16. Thompson KH, Chiles J, Yuen VG, Tse J, McNeill JH, Orvig C. Comparison of anti-hyperglycemic effect amongst vanadium, molybdenum and other metal maltol complexes. J Inorg Biochem 2004;98:683–690. [PubMed: 15134913]
17. Lewis JA, Puerta DT, Cohen SM. Metal complexes of the trans-Influencing ligand thiomaltol. Inorg Chem 2003;42:7455–7459. [PubMed: 14606841]
18. Lewis JA, Cohen SM. Addressing lead toxicity: complexation of lead(II) with thiopyrone and hydroxypyridinthione O, S mixed chelators. Inorg Chem 2004;43:6534–6536. [PubMed: 15476346]
19. Monga V, Patrick BO, Orvig C. Group 13 and lanthanide complexes with mixed O, S anionic ligands derived from maltol. Inorg Chem 2005;44:2666–2677. [PubMed: 15819552]

20. Monga V, Thompson KH, Yuen VG, Sharma V, Patrick BO, McNeil JH, Orvig C. Vanadium complexes with mixed O, S anionic ligands derived from maltol: synthesis, characterization, and biological studies. Inorg Chem 2005;44:2678–2688. [PubMed: 15819553]
21. Lewis JA, Tran BL, Puerta DT, Rumberger EM, Hendrickson DN, Cohen SM. Synthesis, structure and spectroscopy of new thiopyrone and hydroxypyridinethione transition metal complexes. Dalton Trans 2005:2588–2596. [PubMed: 16025179]
22. Jones AG, Abrams MJ, Davison A, Brodack JW, Toothaker AK, Adelstein SJ, Kassis AI. Biological studies of a new class of technetium complexes: the hexakis(alkylisonitrile)technetium(I) cations. Int J Nucl Biol 1984;11:225–234.
23. Marmion ME, Woulfe SR, Neumann WL, Nosco DL, Deutsch E. Preparation and characterization of technetium complexes with Schiff-base and phosphine coordination. 1. Complexes of technetium-99g and -99m with substituted $acac_2$en and trialkyl phosphines (where $acac_2$en = N, N′-ethylenebis[acetylacetone iminatol]). Nucl Med Biol 1999;26:755–770. [PubMed: 10628555] references therein
24. Tisato F, Maina T, Shao LR, Heeg MJ, Deutsch E. Cationic $[^{99m}Tc^{III}(DIARS)_2(SR)_2]^+$ complexes as potential myocardial perfusion imaging agents (DIARS = o-phenylenebis(dimethylarsine); SR^- = thiolate). J Med Chem 1996;39:1253–1261. [PubMed: 8632432]
25. Lisic EC, Heeg MJ, Deutsch E. $^{99m}Tc(L\text{-}L)_3^+$ complexes containing ether analogs of DMPE. Nucl Med Biol 1999;26:563–571. [PubMed: 10473196]
26. Jain D. Technetium-99m labeled myocardial perfusion imaging agents. Semin Nucl Med 1999;29:221–236. [PubMed: 10433338]
27. Acampa W, Di Benedetto C, Cuocolo A. An overview of radiotracers in nuclear cardiology. J Nucl Cardiol 2000;7:701–707. [PubMed: 11144485]
28. Beller GA, Zaret BL. Contributions of nuclear cardiology to diagnosis and prognosis of patients with coronary artery disease. Circulation 2000;101:1465–1478. [PubMed: 10736294]
29. Banerjee S, Pillai MRA, Ramamoorthy N. Evolution of Tc-99m in diagnostic radiopharmaceuticals. Semin Nucl Med 2001;31:260–277. [PubMed: 11710769]
30. Llaurado JG. The quest for the perfect myocardial perfusion indicator… still a long way to go. J Nucl Med 2001;42:282–284. [PubMed: 11216527]
31. Mousa SA, Cooney JM, Williams SJ. Flow-distribution characteristics of Tc-99m-Hexakis-2-methoxy-2-methylpropyl isonitrile in animal-models of myocardial-ischemia and perfusion (abstract). J Am Coll Cardiol 1987;9:A137.
32. Piwnica-Worms D, Kronauge JF, Chiu ML. Uptake and retention of hexakis(2-methoxyisobutylisonitrile) technetium(I) in cultured chick myocardial cells: mitochondrial and plasma membrane potential dependence. Circulation 1990;82:1826–1838. [PubMed: 2225379]
33. Carvalho PA, Chiu ML, Kronauge JF, Kawamura M, Jones AG, Holman BL, Piwnica-Worms D. Subcellular distribution and analysis of technetium-99m-MIBI in isolated perfused rat hearts. J Nucl Med 1992;33:1516–1521. [PubMed: 1634944]
34. Crane P, Laliberte R, Heminway S, Thoolen M, Orlandi C. Effect of mitochondrial viability and metabolism on technetium-99m-sestamibi myocardial retention. Eur J Nucl Med 1993;20:20–25. [PubMed: 7678396]
35. Herman LW, Sharma V, Kronauge JF, Barbarics E, Herman LA, Piwnica-Worms D. Novel hexakis (arenisonitriles)technetium(I) complexes as radioligands targeted to the multidrug resistance P-glycoprotein. J Med Chem 1995;38:2955–2936. [PubMed: 7636856]

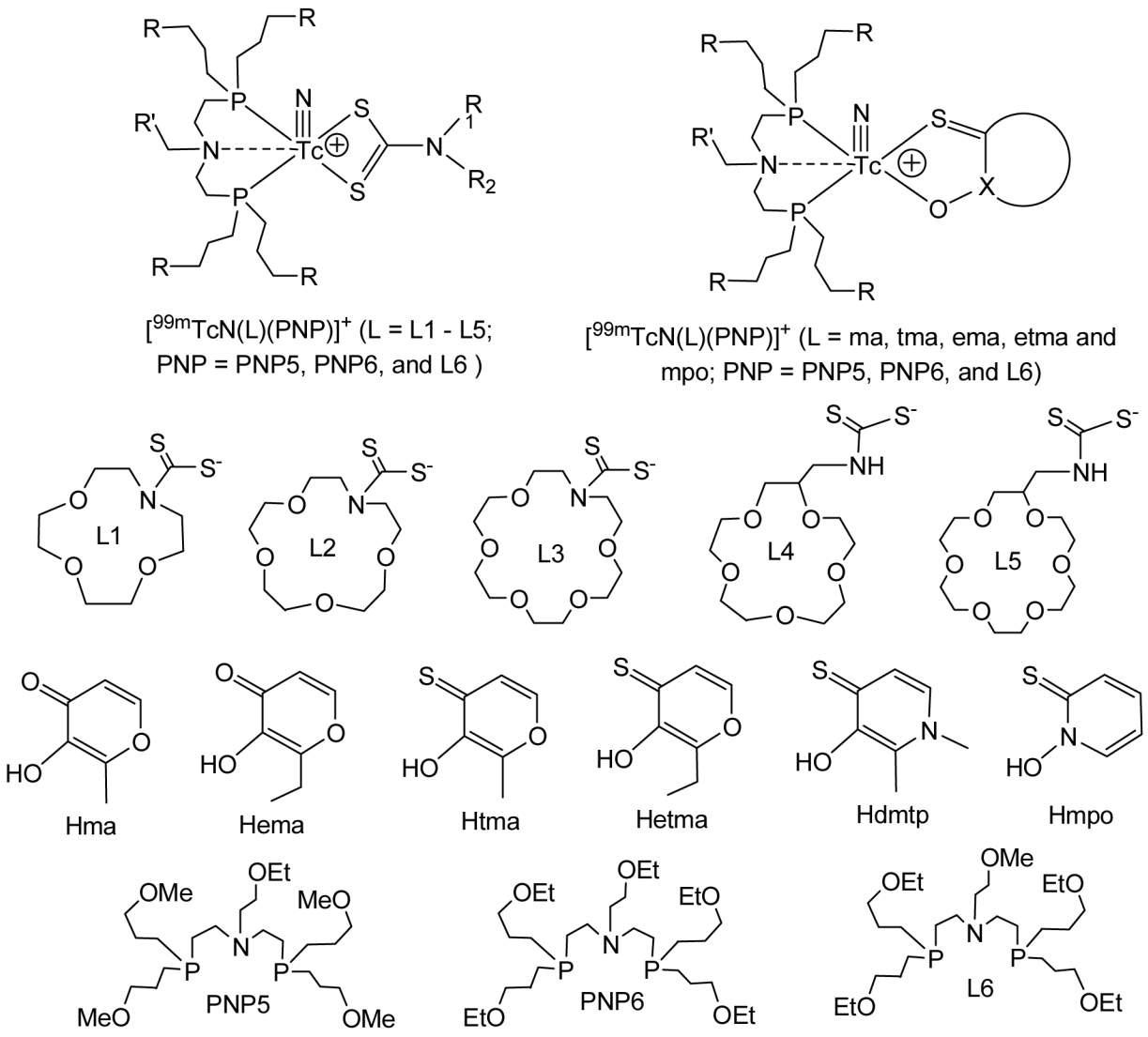

Figure 1.

Bidentate chelators (Hma, Hema, Htma, Hetma, and Hmpo), bisphosphines (PNP5, PNP6 and L6), and their cationic ^{99m}Tc-nitrido complexes [^{99m}TcN(L)(PNP)]$^{+}$ (L = ma, ema, tma, etma and mpo; PNP = PNP5, PNP6 and L6).

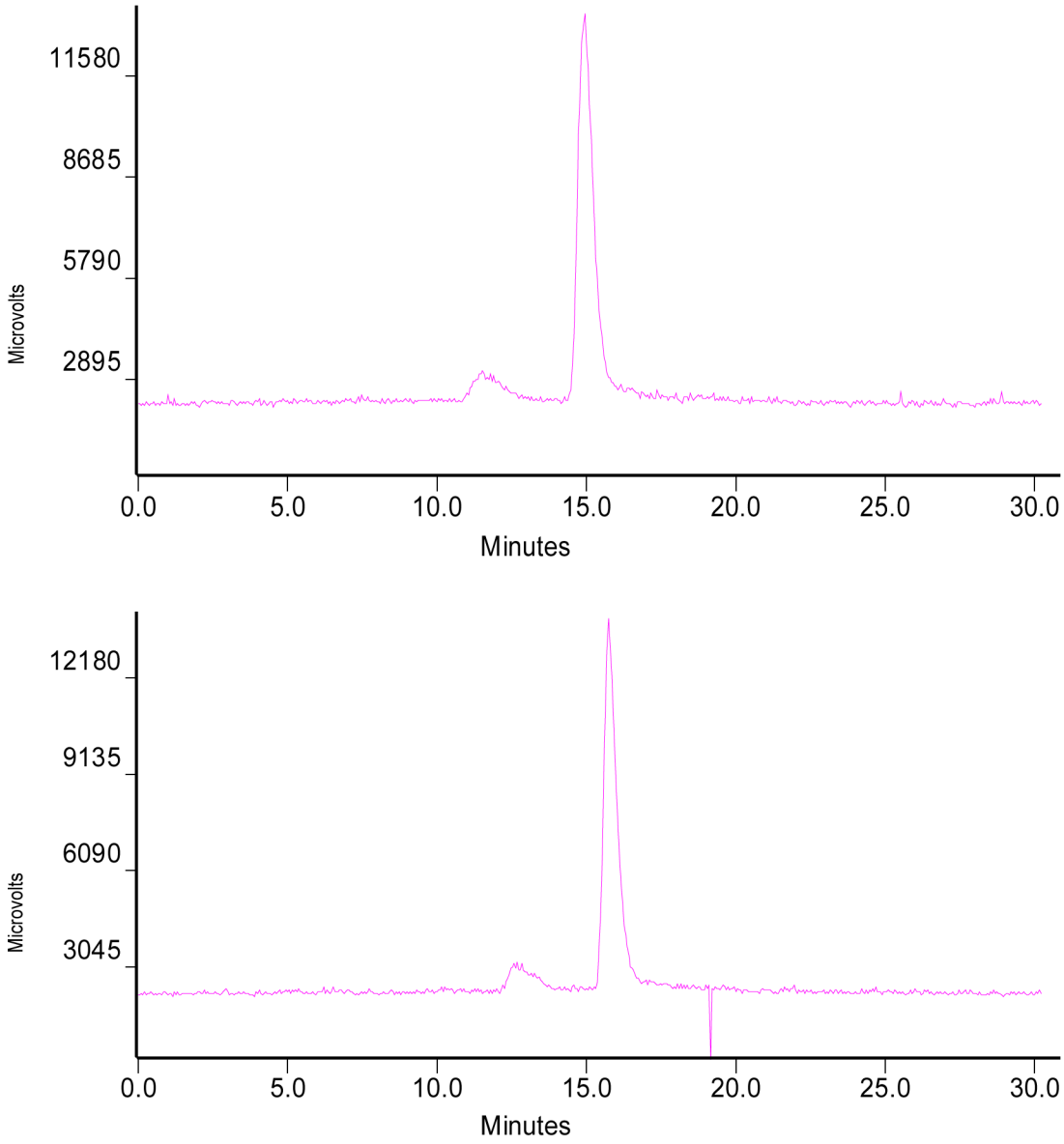

Figure 2.
Typical radio-HPLC chromatograms of $[^{99m}TcN(ma)(PNP6)]^{+}$ (top) and $[^{99m}TcN(ema)(PNP6)]^{+}$ (bottom).

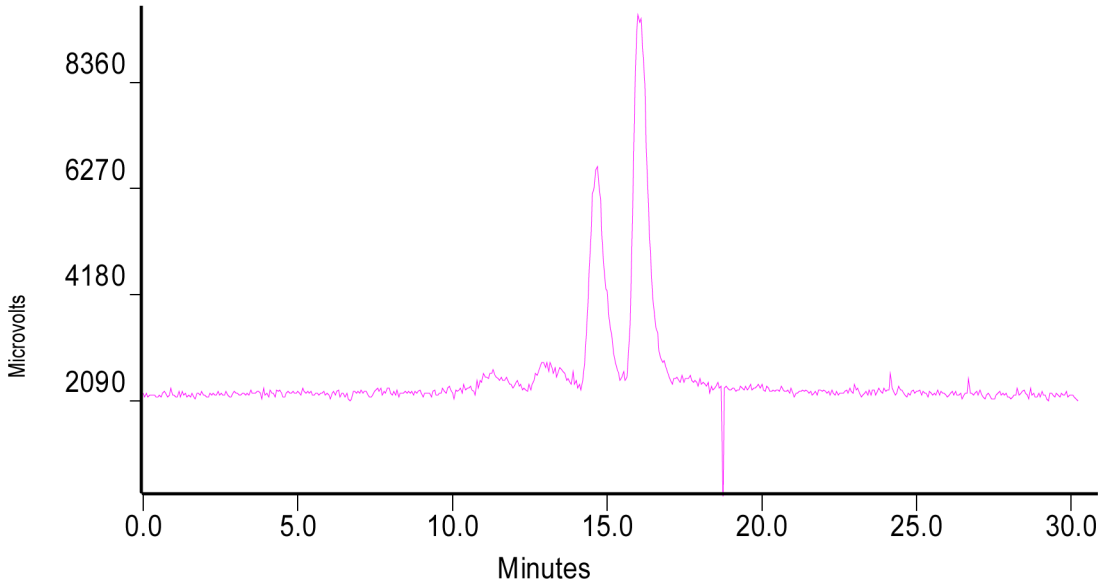

Figure 3.
Radio-HPLC chromatogram of the reaction mixture containing [^{99m}TcN(ma)(PNP6)]$^{+}$ (left) and [^{99m}TcN(ema)(PNP6)]$^{+}$ (right).

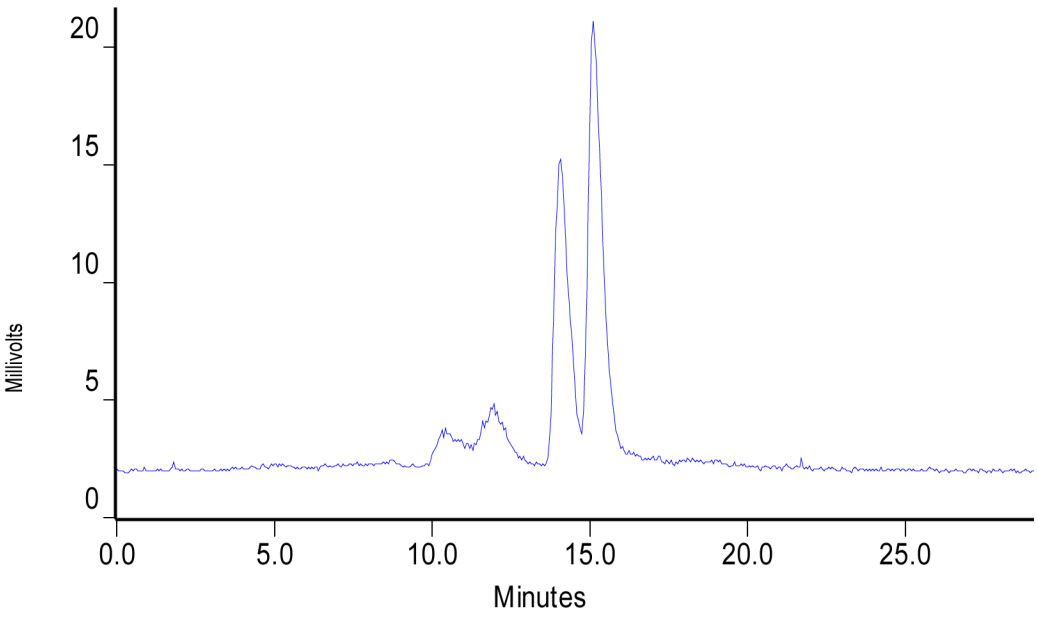

Figure 4.

Radio-HPLC chromatogram of the reaction mixture containing $[^{99m}TcN(ma)(L6)]^{+}$ (left) and $[^{99m}TcN(ma)(PNP6)]^{+}$ (right). The radioimpurities (~20%) at 10 – 12 min are caused by the partial oxidation of PNP6.

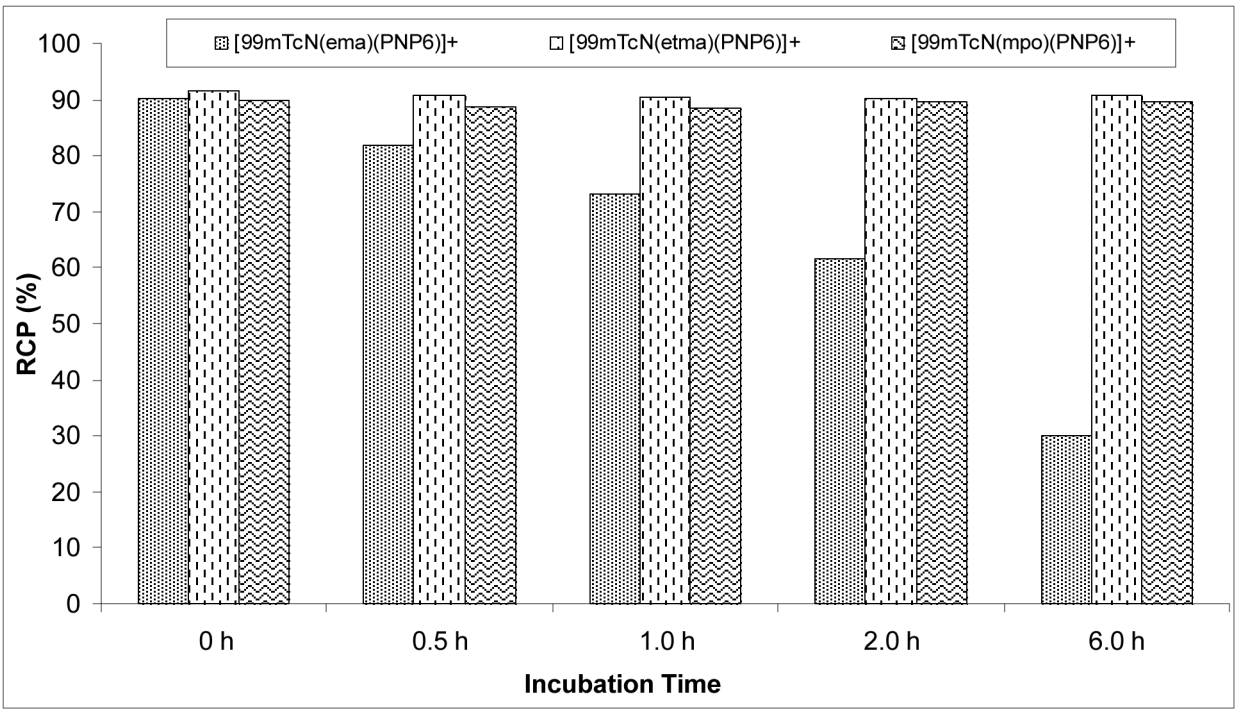

Figure 5.
Solution Stability data for $[^{99m}TcN(ema)(PNP6)]^{+}$, $[^{99m}TcN(etma)(PNP6)]^{+}$ and $[^{99m}TcN(mpo)(PNP6)]^{+}$.

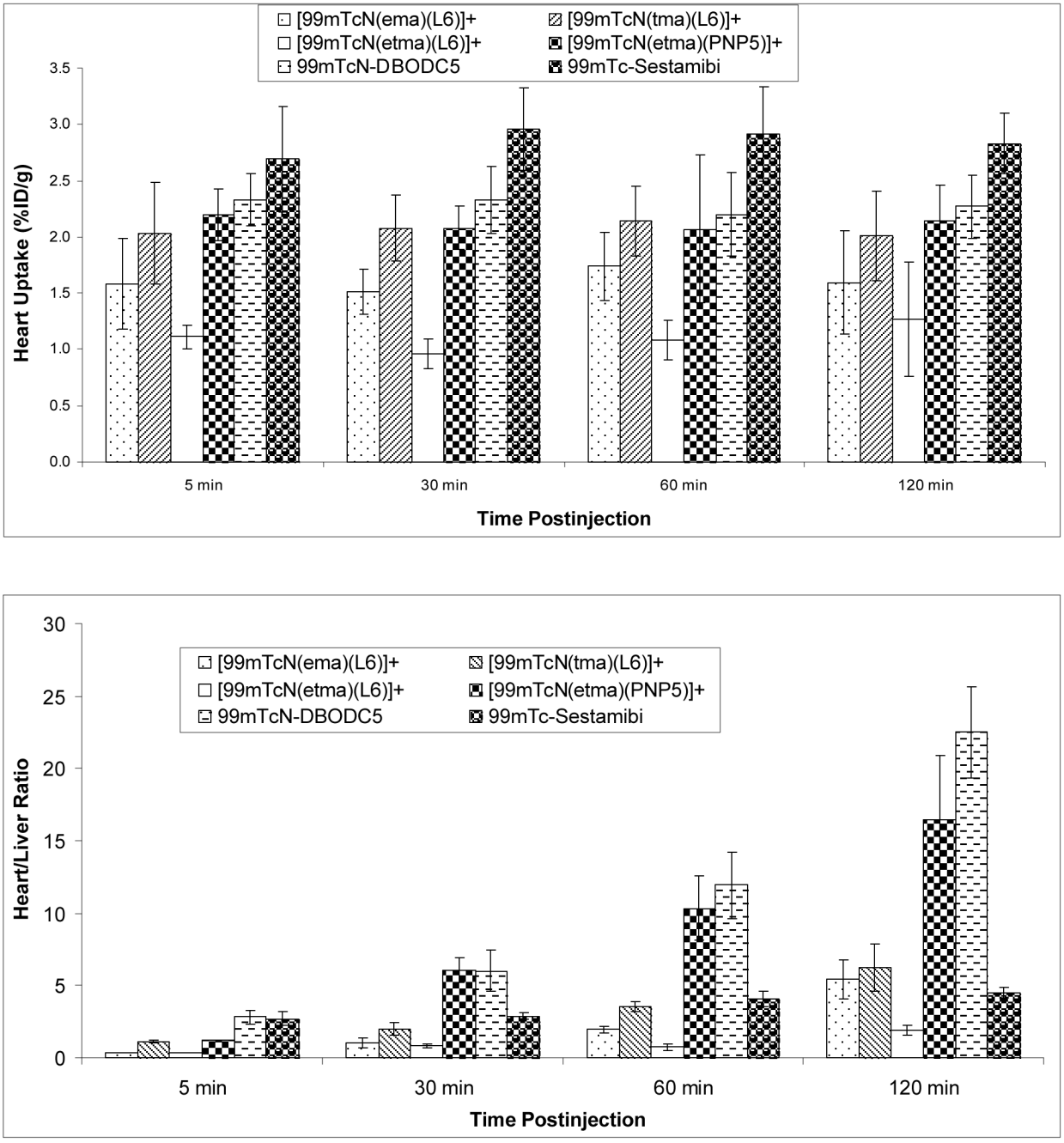

Figure 6.

Comparison of heart uptake (top) and heart/liver (bottom) ratios between [^{99m}TcN(ema)(L6)]$^{+}$, [^{99m}TcN(tma)(L6)]$^{+}$, [^{99m}TcN(etma)(PNP5)]$^{+}$, ^{99m}TcN-DBODC5, ^{99m}Tc-Sestamibi, and [^{99m}TcN(L4)(L6)]$^{+}$.

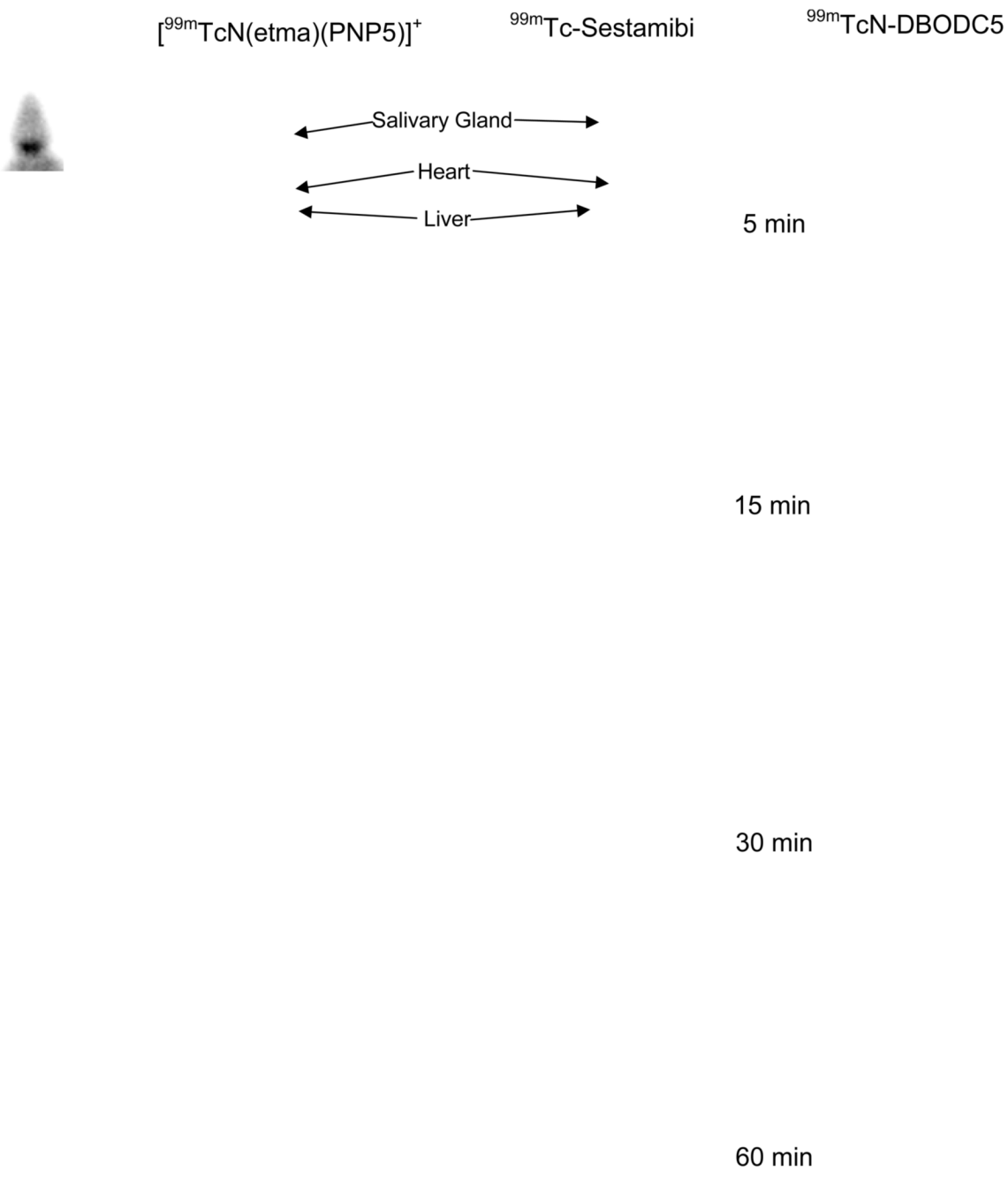

Figure 7.
Planar images of rats administered with ~ 500 μCi of [^{99m}TcN(etma)(PNP5)]$^{+}$, ^{99m}Tc-Sestamibi and ^{99m}TcN-DBODC5. Arrows indicate the location of the heart, liver and salivary gland (as determined by ex-vivo gamma counting).

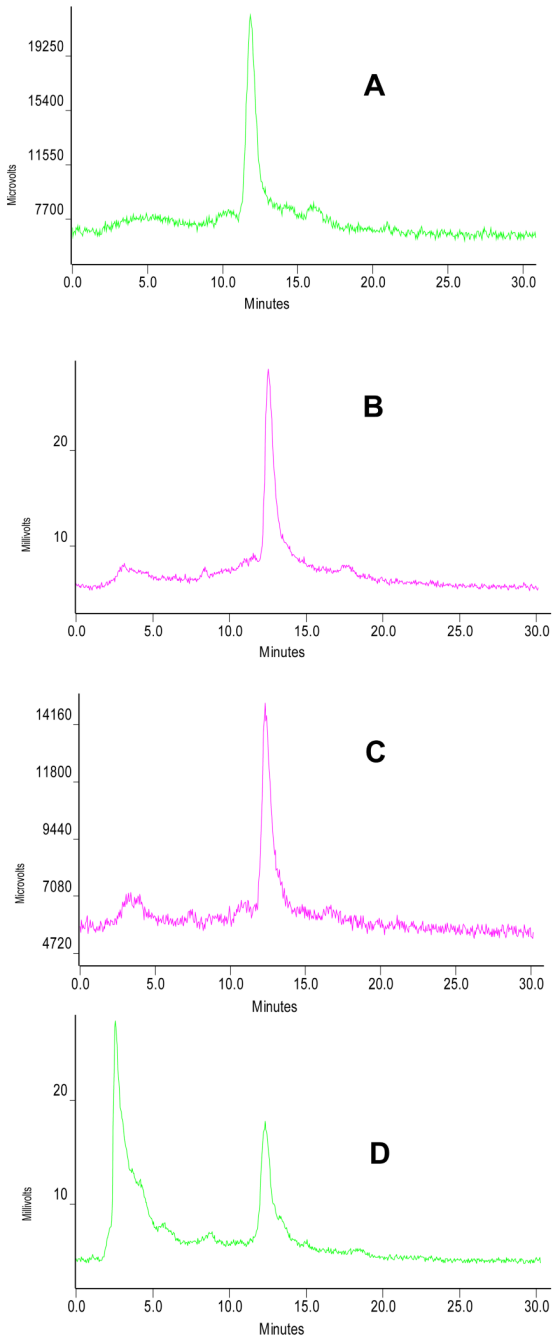

Figure 8.

Radio-HPLC chromatograms of $[^{99m}TcN(etma)(PNP5)]^{+}$ in the kit matrix before injection (A), in the urine at 30 min p.i. (B), in the urine at 120 min p.i. (C), and in feces at 120 min p.i. (D). Each rat was administered with ~500 μCi of $[^{99m}TcN(etma)(PNP5)]^{+}$.

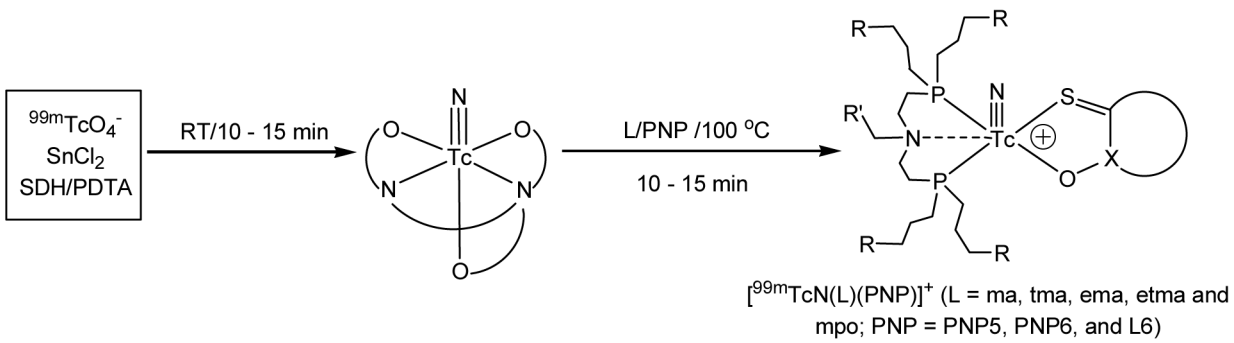

Scheme I.
Synthesis of Cationic Complexes $[^{99m}TcN(L)(PNP)]^+$ (L = ma, ema, tma, etma, and mpo; PNP = PNP5, PNP6 and L6).

Table 1

The RCP data and radio-HPLC retention times of cationic ^{99m}Tc-nitrido complexes.

Compound	Radiochemical Purity (%)	HPLC Retention Time (Min)	Log P Value
^{99m}Tc-Sestamibi	>98%	16.5	1.29±0.15
^{99m}TcN-DBODC5	>90%	16.2	1.10±0.07
$[^{99m}TcN(ma)(PNP5)]^+$	90.5%	9.3	−0.01±0.01
$[^{99m}TcN(ema)(PNP5)]^+$	90.3%	10.7	0.53±0.08
$[^{99m}TcN(tma)(PNP5)]^+$	91.0%	9.9	0.38±0.10
$[^{99m}TcN(etma)(PNP5)]^+$	90.0%	15.5	0.67±0.15
$[^{99m}TcN(mpo)(PNP5)]^+$	91.2%	15.8	0.51±0.05
$[^{99m}TcN(ma)(PNP6)]^+$	91.2%	15.8	1.19±0.13
$[^{99m}TcN(ema)(PNP6)]^+$	90.8%	16.7	1.48±0.02
$[^{99m}TcN(tma)(PNP6)]^+$	85.7%	15.3	1.29±0.02
$[^{99m}TcN(etma)(PNP6)]^+$	92.5%	16.4	1.51±0.01
$[^{99m}TcN(mpo)(PNP6)]^+$	90.3%	16.7	1.49±0.05
$[^{99m}TcN(ma)(L6)]^+$	90.1%	14.2	0.92±0.16
$[^{99m}TcN(ema)(L6)]^+$	90.2%	15.2	1.22±0.13
$[^{99m}TcN(tma)(L6)]^+$	85.8%	15.7	1.09±0.17
$[^{99m}TcN(etma)(L6)]^+$	85.6%	16.6	1.43±0.05
$[^{99m}TcN(mpo)(L6)]^+$	90.3%	13.4	1.32±0.13